Correlation between surface charge and hydration on mineral surfaces in aqueous solutions: A critical review

Hong-liang Li, Wen-nan Xu, Fei-fei Jia, Jian-bo Li, Shao-xian Song, and Yuri Nahmad

View the article online at SpringerLink or IJMMM Webpage.

Articles you may be interested in

Wei Liu, Qing-he Zhao, and Shuan-zhu Li, Relationship between the specific surface area of rust and the electrochemical behavior of rusted steel in a wet-dry acid corrosion environment, *Int. J. Miner. Metall. Mater.*, 24(2017), No. 1, pp. 55-63. https://doi.org/10.1007/s12613-017-1378-5

Xiang-hui Tian, Da-zhao Song, Xue-qiu He, Hui-fang Liu, Wei-xiang Wang, and Zhen-lei Li, Surface microtopography and micromechanics of various rank coals, *Int. J. Miner. Metall. Mater.*, 26(2019), No. 11, pp. 1351-1363. https://doi.org/10.1007/s12613-019-1879-5

Peng Fei, Yi Min, Cheng-jun Liu, and Mao-fa Jiang, Effect of continuous casting speed on mold surface flow and the related near-surface distribution of non-metallic inclusions, *Int. J. Miner. Metall. Mater.*, 26(2019), No. 2, pp. 186-193. https://doi.org/10.1007/s12613-019-1723-y

Venkateswarlu Badisha, Shabana Shaik, Ravikumar Dumpala, and B. Ratna Sunil, Developing Mg–Zn surface alloy by friction surface allosying: *in vitro* degradation studies in simulated body fluids, *Int. J. Miner. Metall. Mater.*, In press. https://doi.org/10.1007/s12613-020-2053-9

Mohammad A. Omari, Hamzah M. Mousa, Faris M. AL-Oqla, and Mohammad Aljarrah, Enhancing the surface hardness and roughness of engine blades using the shot peening process, *Int. J. Miner. Metall. Mater.*, 26(2019), No. 8, pp. 999-1004. https://doi.org/10.1007/s12613-019-1818-5

IJMMM WeChat   QQ author group

Invited Review

Correlation between surface charge and hydration on mineral surfaces in aqueous solutions: A critical review

Hong-liang Li[1,2]*, Wen-nan Xu*[1]*, Fei-fei Jia*[3]*, Jian-bo Li*[1]*, Shao-xian Song*[3]*, and Yuri Nahmad*[4]

1) College of Mining Engineering, Taiyuan University of Technology, Taiyuan 030024, China
2) Department of Chemical and Materials Engineering, University of Alberta, Edmonton, Alberta T6G2V4, Canada
3) School of Resources and Environmental Engineering, Wuhan University of Technology, Wuhan 430070, China
4) Instituto de Fiscia, Universidad Autonoma de San Luis Potosi, Av. Sierra Leona, San Luis Potosi 78000, Mexico

Abstract: Surface charges and hydration are predominant properties of colloidal particles that govern colloidal stability in aqueous suspensions. These properties usually coexist and interact with each other. The correlation between the surface charge and hydration of minerals is summarized on the basis of innovative experimental, theoretical, and molecular dynamics simulation studies. The factors affecting the adsorption behavior of ions and water molecules, such as ion concentration, ion hydration radius and valence, and surface properties, are discussed. For example, the hydration and adsorption states completely differ between monovalent and divalent ions. For ions of the same valence, the effect of surface charge on the hydration force follows the Hofmeister adsorption series. Electrolyte concentration exerts a significant effect on the hydration force at high ion concentrations. Meanwhile, the ion correlations in high-concentration electrolyte systems become long range. The interfacial water structure largely depends on surface chemistry. The hydration layer between different surfaces shows large qualitative differences.

Keywords: surface hydration; surface charged ion; mineral; water molecule

1. Introduction

Stability is a major characteristic of colloid suspensions, which are useful in a wide range of engineering fields related to colloid science, such as mineral industry, hydrometallurgy, material science and engineering, environmental control, wastewater treatment, nanotechnology, pharmaceutical industry, and biotechnology [1]. This characteristic is determined by the energy barrier between pairs of particles, which prevents their agglomeration. The energy barrier is governed by the charge and hydration on the particle surface. Investigations of surface charge and hydration are important in colloid science. In general, the surface charge and hydration of a particle surface form simultaneously. Thus, understanding the correlation between them is significant.

Charged ions, surface hydrated water molecules, and ion hydrated water molecules simultaneously form on a particle surface. Fig. 1 presents the schematic of the surface charge and hydration of a hydrophilic particle surface. The adsorbed water molecules and ions form the ordered and transition layers on the surface. Surface hydration has two major parts: particle surface hydration and ion hydration. Turbidity remains high even around the isoelectric point (IEP), indicating that colloidal particles remain inherently stable. This phenomenon verifies the existence of a surface hydration layer coating the particles [1]. In addition, grand canonical Monte Carlo (GCMC) simulations showed that five water molecules surround the Na^+ cation on the montmorillonite surface, suggesting the existence of ion hydration on the surface. The other cations are also hydrated in bulk water; for example, the coordination numbers of Na^+, K^+, Mg^{2+}, and Ca^{2+} are 5.6, 6.7, 6.0, and 7.8, respectively [2].

Surface-adsorbed ions and water molecules interact with each other in the ordered layer and transition layer. The adsorbed ions form the Stern layer and its defused layer. Meanwhile, the adsorbed water molecules form the hydration layer and its defused layer. The relationship among charged ions, surface hydrated water molecules, and ion hydrated water molecules is complicated. However, the interaction between surface charge and hydration is difficult to detect,

≰ Springer

858

Int. J. Miner. Metall. Mater., Vol. 27, No. 7, Jul. 2020

and the hydration structures adjacent to particle surfaces and ions are complex. Competition occurs between the adsorbed water molecules and the ions on the surface; moreover, surface hydration can be enhanced by the adsorption of hydrated ions. In addition, the adsorption behavior differs between various types of surfaces and ions. Therefore, the investigation of the relationship between surface charge and hydration is challenging.
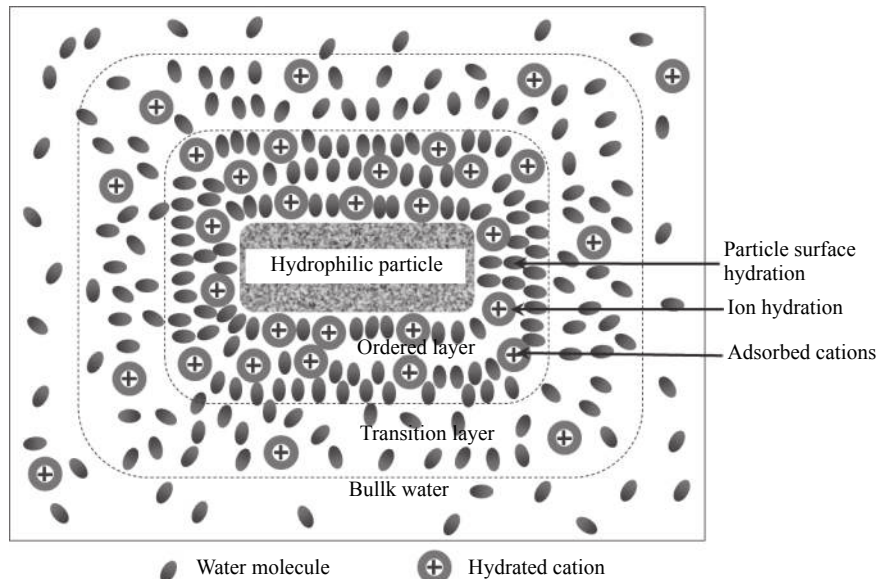

Fig. 1. Three-structure model of surface charge and hydration on a hydrophilic surface [3].

Many articles focused on surface charge and hydration. This review presents a comprehensive appraisal of available information to provide a systematic evaluation of the study methods for surface charge and hydration to clarify the relationship between surface charge and hydration. First, the relationship between surface charge and hydration is discussed. Afterward, the experimental, theoretical, and simulation studies employed to characterize surface charge and hydration are provided. Then, the main factors influencing surface charge and hydration behavior are discussed. These factors include surface structure, cation valence, hydrolysis species, and cation concentration. Finally, the effects of ion hydration on surface hydration and charge are considered. This review illustrates some common minerals or material surfaces, such as quartz, kaolinite, montmorillonite, and mica, to expound on surface charge and hydration from the mineral or material perspective.

2. Interactions between surface charge and hydration

2.1. Effects on surface charge and hydration

Interactions occur between surface charge and hydration. The adsorption of hydrogen ions does not give rise to hydration forces [4] but affects the surface potential; the more acidic IEPs observed with increasing hydration probably reflect the increasing replacement of OH$^-$ by Cl$^-$ [5]. The ion hydration effect on the surface can arise from the adsorption of cations. However, the effect of counterion hydration varies between different surface structures. For example, the hydration force on the surface of mica originates from the dehydration of cations [6]. Overlap of the ion hydration shell exists [4]. The coagulation can be destroyed by this cation hydration during the overlap of the double layers when the cation concentration is high. The difference between multivalent cations is that the hydration shell of higher valence cations is stronger and harder to shed during adsorption [7]. On the surface of silica, the hydration force decreases with increasing counterion hydration degree [8].

Competition occurs between the formation of the hydration layer and the ion layer adjacent to the surface at a high electrolyte concentration [9]. The influence of the surface charge on the hydration layer originates from the external electric field of ions. When the electric field is greater than 0.25 V/nm, the influence of ions on the hydration layer must be considered. The effects of ions on surface hydration typically follow the Hofmeister series [10], and the placement of ions on the surface correlates with this series. Ion hydration decreases the differential capacitance of the hydration layer on the surface [11]. However, hydration also has a complex effect that squeezes out the ions because of the overwhelmingly large number of water molecules [12]. Regarding the effect of positive charge on hydration, an increase in monovalence and bivalence cation charge is suggested to significantly decrease the size of the first surface hydration shell.

The effect of surface charge on hydration depends on the

hydrolysis of surface and cations, which is pH dependent. Vibrational sum-frequency generation spectroscopy results show that the maximum perturbation by salt at the silica/water interface occurs at pH value 7–8, suggesting that the maximum influence of salt on the molecular arrangement of water at the surface occurs at pH value 7–8 [13]. If M^{Z+} behaves as hydrated ions, hydrolyzed multivalent metal ions can be characterized as $[MO_nH^{2n-h}]^{(Z-h)+}$, where n is the number of water molecules in the hydration shell and h is the number of protons lost from the hydration shell. The hydrated hydrolyzed forms of cations include aquo, hydroxoaquo, hydroxo, oxohydroxo, and oxo forms [14]. This hydrolysis behavior largely affects surface hydration.

Regarding the effect of negative charge on hydration, the inner layer hydration repulsion is dominated by interfacial water, whereas the outer hydration is dominated by the anionic layer. The ion hydration structure is dependent on anions with different hydration energies. For anions with low hydration energies, a significant degree of ion-water structuring occurs because of the specific adsorption effects within the Stern layer. By contrast, ions with high hydration energy are less structured in the Stern layer [15]. Compared with the positively charged surface, a water molecule shows fewer and weaker hydrogen bond between water and the delocalized π orbitals surface (π–H bond) with negative charge [16].

The effect of surface hydration on charge is mainly embodied in the simultaneous competition and collaboration between the particle surface charge and hydration. The formation rate of the electrical double layer (EDL) increases with increasing ion concentration and decreasing dielectric constant of the solution [9], which means that the charge effect becomes greater than that of hydration. The order of the adsorption energy of calcium ions and water molecules on the (001) and (010) surfaces of montmorillonite is $CaOH^+ > Ca^{2+} > H_2O$ in aqueous solutions [17]. Meanwhile, Peng *et al.* [17] found that the surface charge and surface hydration can also be enhanced by each other. The adsorption energy of Ca^{2+} and $CaOH^+$ on the Na-montmorillonite (001) surface is increased from −36.5 to −72.1 kJ/mol and from −126.9 to −154.8 kJ/mol by the effect of surface hydration, respectively. The corresponding adsorption energy of water molecule on the quartz (001) surface increases from ∼−72.60 to −172.56, −131.32, and −173.36 kJ/mol with the adsorption of Na^+, Mg^{2+}, and Ca^{2+}, respectively [18].

Correspondingly, Derjaguin–Landau–Verwey–Overbeek (DLVO) theory should be modified because of the additional effect of the hydration layer. Van Oss *et al.* [19] proposed that in addition to Lifshitz–van der Waals (G_{LW}) and short range contributions (G_{SR}) caused by hydrogen bonding between two surfaces must also be considered. The inclusion of the hydration energy (G_{HE}) led to the development of the extended DLVO (EDLVO) theory, which can be used to predict the adhesion of two particles. In specific, the reversibility of EDLVO predictions is more accurate than that of DLVO predictions [20].

2.2. Effect of ion hydration on particle surface hydration

Previous studies indicated that surface hydration can be enhanced by ion hydration. For example, rheological test results suggested that surface hydration can be greatly enhanced by binding hydrated cations (Na^+ or Ca^{2+}) on the silica/water interface in a NaCl or $CaCl_2$ solution [3,21]. Pashley [4] detected the hydration forces between two molecularly smooth mica surfaces. Results showed that the hydration forces apparently increase when the mica surface is adsorbed with hydrated cations. The exponential "hydration" force decay length is 1.0 ± 0.2 nm for the mica interaction when the surfaces are completely adsorbed with K^+ and Na^+ ions. Short-range repulsive hydration forces between surfaces (especially for the 2:1 clay minerals which has the crystal structure of 2 silicon–oxygen tetrahedron layer sandwiches with 1 aluminum–oxygen octahedron layer) appear with the adsorption of hydrated cations [4]. GCMC, molecular dynamics (MD) simulation, and periodic density functional theory (DFT) results suggested that ion hydration plays a dominant role on (1) montmorillonite and (2) beidellite (001) surface hydration [22–23]. Interactions between the 2:1 layer surfaces and water molecules are much weaker than that of adsorbed cations [24–25]. The binding between Na (of Na^+) 3s and O (of water molecule) 2p ranges from −5 to −0 eV, and the anti-bonding between Na 3s and O 2p orbitals ranges from of 5 to 8 eV [23]. The effects of ion hydration on surface hydration are summarized as follows.

First, the effect of ion hydration on surface hydration depends on the chaotropic activity of the ions. Measurement of the surface force between mica surfaces revealed that surface hydration is induced by the strongly hydrated cosmotropic ions. The weakly hydrated chaotropic ions tend to be excluded from the surface hydration layer [26].

Second, the effect of ion hydration on surface hydration also depends on the valence and ratio of the adsorbed ions. As the ion valence increases or the ratio decreases, the magnitude of the hydration force increases and the decay length decreases [27], and then the hydration ability increases [24]. For example, the hydration layers of montmorillonite and kaolinite are thicker in Na^+ solutions than in Ca^{2+} solutions [28]. The hydration ability of the cations follows the order $K^+ < Na^+ < Ca^{2+} < Mg^{2+}$ on the (001) surface of montmorillonite [24–25]. Monovalent ions adsorb in an incomplete hydrated state and partly neutralize the surface charge. Divalent ions are adsorbed in completely and incomplete hydrated states while achieving complete charge compensation [29].

For ions of the same valence, comparison of the hydration forces in the presence of various alkali chloride salts revealed that the effect of surface charge on the hydration force follows the Hofmeister adsorption series [30], except for K^+.

The electrosorption capacity for anions and cations has a negative linear relationship with the hydration ratio [31]. The K^+ anomaly is attributed to the small ion size and weakly hydrated chaotropic effect [32].

Third, ion concentration plays an important role in surface hydration. Veeramasuneni *et al.* [33] measured the forces between silica surfaces in solutions with high ionic strength through atomic force microscopy (AFM). At high ion concentrations (>3 mol/L) for divalent cations, the electrostatic force can be completely ignored [34]. Meanwhile, the hydration force is significantly affected by the electrolyte concentration at high ion concentrations. However, at low ion concentrations, the effect of electrolyte concentration (up to 0.1 mol/L) on the hydration layer force can be neglected [35].

2.3. Effect of ion hydration on surface charge

The influence of ion hydration on surface charge is commonly called the specific ion effect. It can be detected using AFM based on a π-transition phenomenon, in which a stepwise decrease in the pull-off force can be measured over a narrow range of salt concentrations [36]. The ion hydration structure exerts a great effect on the adsorption of ions on the surface. For example, weakly hydrated ions can condensate onto the mica lattice, shielding the whole surface charge in the Stern layer. By contrast, strongly hydrated Li^+ only incompletely neutralizes the surface charge in the Stern layer, resulting in the formation of a diffused layer [37]. The specific volume of the adsorbed water has a great effect on the exchanged ions as the ions are exchanged in the pores of the hydration layers [38].

The effect of ion hydration increases the volume of the counterions that influence the surface charge. The ion hydration effects can be typically ordered in series, and the placement of ions in this series correlates well with the hydration properties of the ions in bulk water [39]. Under some conditions, the hydration of ions affects the repulsive force between the two plates, and the sequence of its strength follows closely the Hofmeister series [40]. To include the cation hydration volume in double-layer theory, Pashley [4] modeled the surface charging/ion-exchange properties of mica by using a simple mass action (site-binding) theory where hydrated ion sizes are included. Then, Miklavic and Ninham [41] updated a further lattice model to describe the competition adsorption of two species in different hydration volumes accurately.

The equation of state about "Boublik–Mansoori–Carnahan–Starling–Leland" has been included in Poisson–Boltzmann (PB) theory to describe the volume interactions in ion hydration [42]. The modified equation can be in good agreement with the experimental data as the hydrated size of the divalent ion is used, even when all spheres have very small radii and do not differ by more than 0.1 or 0.2 nm, near the plane of high charge (e.g., 600 mC/m^2).

3. Surface charge

The study of surface charge mainly includes the following three parts: experiments, PB theory, and MD simulation. The electrostatic force, distribution of the electric potential, and surface charge structure can be investigated by AFM and scanning force microscopy (SFM) [34,43], PB theory [44], and MD simulation, respectively. These studies are summarized as follows.

3.1. Experimental research on surface charge

3.1.1. Methods

The electrostatic force of the surface charge can be detected by AFM [34,43]. The electrostatic force (F_c) can be approximated by the following equation [34]:

$$F_c = \frac{4\pi}{\varepsilon_0 \varepsilon \kappa^2} \left[g_1 \left(\sigma_T^2 + \sigma_S^2 \right) e^{-2D\kappa} + g_2 \sigma_T \sigma_S e^{-D\kappa} \right] \qquad (1)$$

where σ_T and σ_S are the charge densities of the tip and sample surface, ε_0 and ε represent the vacuum permittivity and the dielectric constant of water, D is the distance between the tip and the sample, g_1 and g_2 are geometry factors that only depend on the tip shape, and κ is the inverse of the Debye length. Basing from this equation, Sotres *et al.* [45] presented a method to image a specimen in aqueous media through AFM without establishing any mechanical contact between the tip and the sample. It works by setting the feedback set point to just before mechanical instability occurs in the repulsive EDL force curve. Then, the repulsive EDL force of the specimen is mapped with jumping mode operation. The height difference of adsorbed molecule and the Debye length exhibits a linear relationship, which is in good agreement with theory.

Furthermore, Heinz and Hoh [46] developed another experimental method called D (distance)–D mapping for generating relative surface charge density maps by using AFM. D–D mapping correlates the force distribution of surface charge between two surfaces in different vertical distances. The advantage of D–D mapping is that it is independent from parameters such as tip–sample contact point, cantilever spring constant, tip radius, and surface charge density of tip. The surface charge density can also be detected using SFM. The surface charge density of the test sample can be derived with a known charged alumina by comparing the electrostatic forces measured on two substances. Using this method, Heinz and Hoh estimated the charge density of purple membranes to be −0.05 C/m^2 [46].

3.1.2. Applications

AFM results show that the thickness of the compact part of the double layer is probably slightly less than 1 nm, which is equal to the thickness of three water molecules for the water layer. The thickness of the inner part of the compact layer is equal to the radius of a hydrated ion (0.35 ± 0.05 nm) [47].

AFM and SFM are special techniques for measuring the surface charge of particle surfaces with different chemical compositions, such as the basal and edge surface of clay particles. Yin *et al*. [48] measured the basal and edge surface forces of kaolinite. Results illustrated that the silica tetrahedral face is negatively charged if pH value >4, whereas the alumina octahedral face is positively charged if pH value <6 and negatively charged if pH value >8. Using SFM method, Liu *et al*. [49] detected the basal and edge surface forces of kaolinite. The measured surface forces can be well fitted using classic DLVO theory. The edge surface has a point of zero charge below pH value = 4. AFM measurements also suggested that the alumina octahedral layer of kaolinite exerts minimal influence on the edge surface charge possibly because of the lack of isomorphous substitution in the tetrahedral layer structure.

AFM is also a special technique for detecting the surface charge when counterions are monovalent and divalent ions. Classical DLVO theory is only applicable for the adsorption of multivalent ions. Other attractive forces are attributed to surface charge heterogeneities for monovalent and divalent ions, which results in higher stability ratios from direct force measurements than experimental values and reverse the potential [50]. These attractive forces can be measured by AFM. Ionic correlations are also the main factor for surface force because they cause charge inversion and enhance the heterogeneity of surface charges [51].

3.2. Theoretical and simulation research on surface charge

3.2.1. Poisson–Boltzmann theory

PB theory is widely used to obtain insights into charged colloid systems and to elucidate the fundamental properties of charged surfaces. It is based on two main assumptions: (i) ion–ion correlations are neglected [52–54] and (ii) charge carriers are infinitely small point charges [55]. PB theory is considered an exact theory for low valence ions at low or even moderate electrolyte concentrations of bulk solution with ionic strength lower than 0.1–0.5 mol/L because of the small influence of ionic volume effects and the dispersion forces on it [44,56]. The effect of hydration on the surface charge should be considered in this theory.

Many researchers have been dedicated to studying PB-related features and to experimentally confirming them. For example, Borukhov *et al*. [55] developed a modified PB theory that considers the volume excluded by the ions to explain the size effect of ion hydration. In this modified equation, a simple expression for steric effects including surface charge density and ion size effect is derived. Meanwhile, Alijó *et al*. [57] developed a mathematical structure by differential algebraic to solve the size effects of the double layer interaction between two charged plates. In this method, several ion charges on the interfaces are modeled by the density profiles under the immersion of various aqueous electrolyte solutions.

To describe the adsorption of counterions on a surface, Gouy and Chapman analyzed the PB equation by using a model of a charged planar particle surrounded by point electrolyte ions in a uniform dielectric continuum solvent [15]. The primitive Gouy–Chapman theory entirely neglects any ionic characteristics but its valence. Ben-Yaakov and Andelman [58] studied the effect of charge boundaries on the pressure between two plate-like particles. The boundary conditions can be used to calculate the dissociation of surface charge groups as a function of separation.

The electrical potential and the energy between two plate-like, cylindrical, and spherical particles were investigated to study the PB equation for different shape particles [59]. The obtained results are reasonably accurate if the diameter of the particle exceeds five times the thickness of the electric double layer. Meanwhile, it still appears as a satisfactory theory during the surface potential and/or the counterion valence is sufficiently high. However, these theories might hardly apply to practical interest. A general expression of the potential of these particles is highly desirable. In this case, a perturbation solution was derived based on the curvature of the particle surface [60]. The results indicate that the solutions are applicable in a wide magnitude of the surface potential and counterion valence. The accuracy increases with the surface potential and/or the counterion valence.

The surface potential pattern affects the surface charge on the decay. For example, the interaction between spheres with a periodic potential decays faster than that between spheres with a uniform potential. Stankovich and Carnie [61] derived a further PB model extension that considers the "random" surface potentials. Then, the Deryaguin approximation of single-mode spheres was obtained, and the force and torque of particles on each other were calculated. Many of the concepts developed from the periodic potential models are useful.

A complete understanding of the physical and chemical processes in diffused EDL requires correct mathematical descriptions and accurate solutions. Then, various approximate solutions methods of the PB equation have been studied. For example, Wang *et al*. [62] developed a lattice evolution solver of the PB equation in confined domains, particularly the nonlinearized PB equation for different types of boundary conditions. This lattice evolution solver is competent for complex geometry conditions and easy extension to 3D cases. To extend the limitation ranges of particle separations, Liu and Neretnieks [63] derived an approximate expression for the force between two parallel plates over a wide range of plate separations, which is in good agreement with the complex exact analytical solution for two plates with constant surface charge densities immersed in a symmetrical electrolyte solution. The advantage of the new method is its fast

convergence of atomic forces at coarse grid spacing.

3.2.2. Simulation and theoretical studies on surface charge beyond the classical PB theory

PB theory has been patched in the past by including a term that considers the ionic volume with some success, as discussed above. However, this approach does not include (1) ion correlations and ionic excluded volume effects on the force between charged surfaces in the presence of monovalent and divalent electrolytes [64], (2) long-range interactions between ions and colloidal surfaces due to ion correlations [65], (3) effects due to different degrees of ionic hydration in the EDL and the associated impact in the potential of mean force among charged colloidal particles [66–75], and (4) an induced effective ionic size asymmetry in equally sized electrolytes due to polarization effects [76]. All of these effects have been studied theoretically and via computer simulations.

Integral equations theory (IET) and MC simulations have demonstrated that counterions do not dominate the electrical properties of a spherical macroion in the presence of unequally sized ions, symmetric in valence, if ion correlations and ionic excluded volume effects are considered consistently. To analyze ion correlations, Kjellander *et al.* [64] performed theoretical anisotropic hypernetted chain calculations and MC simulations of the EDL associated with monovalent and divalent aqueous electrolyte surrounding two charged plates. This study showed that the surface interaction between equally charged plates for 1:1 electrolytes is repulsive except at high salt concentrations, showing a weak attractive minimum. For divalent counterions, the surface interaction between equally charged plates displays an attractive minimum at short separations. Such a minimum becomes more attractive when the electrolyte concentration is increased, but this interaction becomes oscillatory at larger separations. Ion correlations promote a long-range attraction among equally charged colloids functionalized with DNA strands in the presence of monovalent and divalent aqueous electrolytes at high salt concentrations, as demonstrated via experiments, MD simulations, and theory [65]. To study the effects of different degrees of ionic hydration in the EDL and the associated potential of mean force, researchers [66–69] have performed several IET calculations and MC and MD simulations. On the basis of the hypernetted chain/mean spherical approximation (HNC/MSA) integral equation, a more realistic description of the size-asymmetric EDL was provided. Compared with traditional mean-field theories, such as the modified Gouy–Chapman and the unequal radius modified Gouy–Chapman, the HNC/MSA approach considers ion correlations and ionic excluded volume effects consistently [66]. According to MC simulations of a spherical macroion immersed in a primitive model electrolyte, the ionic size and the ionic size asymmetry should be considered as sensitive parameters controlling the electrostatic–entropic

coupling in the EDL. The HNC/HNC and the HNC/MSA have shown good concordance with MC simulations [67]. MC simulations confirmed previous theoretical predictions, including the nondominance of counterions in the size-asymmetric spherical EDL, the appearance of anomalous curvatures of the mean electrostatic potential at the outer Helmholtz plane, and the enhancement of the charge reversal and electrostatic screening at high colloidal surface charge densities due to the ionic size asymmetry. In these instances, the ionic size asymmetry can be associated with an effective ionic hydration [68]. In addition, for a given counterion size, the size of co-ions can considerably affect the colloidal charge neutralization and electrostatic screening close to a charged surface in the presence of monovalent ions at high concentrations. Even in the presence of monovalent salts, a rich phenomenology can be found depending on the ionic size and the degree of hydration of each ionic species [69]. An asymmetric charge neutralization and electrostatic screening depending on the charge polarity of a single nanoparticle occur in the presence of size-asymmetric monovalent electrolytes. This behavior significantly affects the effective potential of mean force between two equally charged macroions. MD simulations and IET calculations performed at the McMillan–Mayer level of description have been used to study the associated ion size effects. These calculations go beyond the standard description provided by the well-known DLVO theory [70]. Moreover, MC simulations have been used to study the effect of hydrated ionic sizes, ion correlations, image charges, and polarization, which are not included in the classical nonlinear PB theory. Simulations of the EDL near oil/water interfaces have displayed a rich phenomenology absent in the nonlinear PB theory, including a local amplification and inversion of the electrical field promoted by an unequal degree of ionic hydration in monovalent salts [71–72].

DFT theory has been also used to describe the influence of surrounding ions and model water molecules, including ion correlations, ionic size asymmetry, and excluded volume effects of ions and solvent particles. In specific, the ionic potential of mean force has been analyzed and decomposed theoretically using the DFT approach in different contributions that depend on electrostatic ion correlations and ionic excluded volume effects. An oscillatory behavior of the ionic potential of mean force associated with co-ions is promoted mainly by the solvent hard sphere contribution [73]. Conversely, the theoretical and simulation prediction of the occurrence of the nondominance of counterions through IE theory and MC simulations exhibited a non-monotonic order or precedence of the mean electrostatic potential at the Helmholtz plane of a charged colloid [74]. The ion size effects enhance the colloidal stability of equally charged macroions at high salt concentrations. With the adsorption of large counterions and small co-ions, the enhanced colloidal stability can

be understood in terms of increased short-range electrostatic and steric repulsions arising from a swollen Stern-like layer at high surface charge densities of nanoparticles [75]. Even the integral equation HNC/HNC approach fails to consider quantitatively the potential of mean force. A proper description of this behavior poses a theoretical challenge to be overcome in the future.

The effect of dielectric heterogeneities on the ion distribution close to a charged colloidal surface is also neglected in PB theory. MC simulations help explain the electrostatic screening and charge neutralization near the surface of a dielectric nanoparticle in the presence of multivalent ions. An effective ionic size asymmetry in the presence of equally sized electrolytes can be promoted by polarization effects in weakly charged spherical nanoparticles with low dielectric permittivity [76].

One quantity that naturally arises from the PB theory is the Debye length. This parameter is widely used experimentally to characterize the thickness of the EDL that neutralizes a charged colloidal surface. By definition, the Debye length only depends on the bulk properties of the surrounding electrolyte, such as the numerical bulk concentration, valence, and the dielectric constant and temperature of the solvent. As a result, important physical characteristics of Coulombic systems are neglected in this approach, such as the influence of the colloidal surface charge density, ion correlations, ionic excluded volume effects, and image charge or polarization effects. Recently, a Debye length generalization, which is the so-called "capacitive compactness," has been proposed as a

novel and accurate measure of the spatial extension or thickness of the EDL [77–80]. This quantity, proposed by G.I. Guerrero-García and others, corresponds to the separation distance between two charged plates associated with an effective equivalent capacitor describing the EDL that surrounds a physical electrode. Using this description, studies showed via simulations and theory an anomalous expansion of the EDL in molten salts and aqueous electrolytes when the colloidal surface charge density increases in the presence of multivalent co-ions [77–78].

Thus, computer simulation is a special technique for studying the structure of the EDL. Similar to the AFM results, the MD results also show that the thickness of the compact part is a little less than 1 nm, equivalent to a water layer with the thickness of three water molecules or the radius of a hydrated ion (0.35 ± 0.05 nm) [47].

Computer simulation is also a special technique for measuring the surface charge when the ions and the surfaces have different chemical compositions. Researchers studied the adsorption of yttrium and calcium on different surfaces of kaolinite and Na-montmorillonite by using DFT simulation, respectively [17,81]. The adsorption patterns of yttrium and calcium are shown in Figs. 2 and 3, respectively. Covalent and electrostatic bonding are the main interactions between $Y(OH)_{3-n}^{n+}$ ($n = 1$–3) ions and (001) surface, whereas electrostatic bonding is the only interaction on the $(00\bar{1})$ surface [81]. Meanwhile, $CaOH^+$ has greater adsorption energy on the edge surface of Na-montmorillonite (-328.8 kJ/mol) than on basal surface (-126.9 kJ/mol) [17].
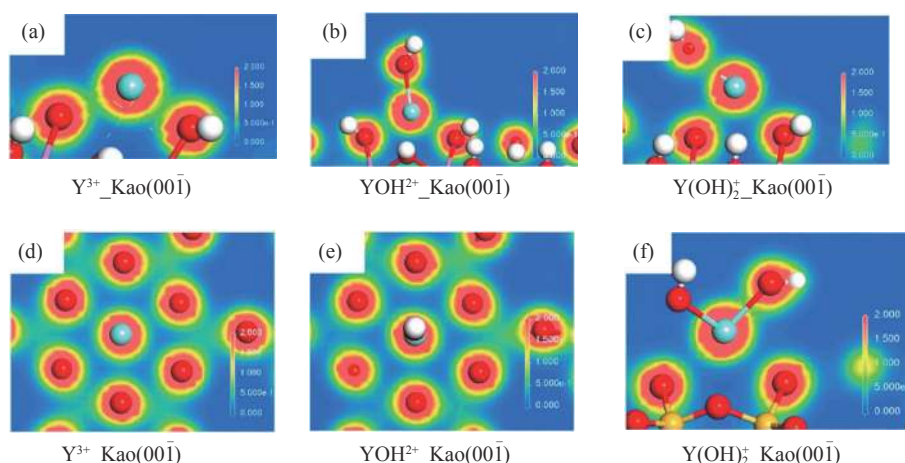
Fig. 2. Electron density pattern of $Y(OH)_{3-n}^{n+}$ ($n = 1$–3) on neutral kaolinite (a)–(c) (001) surface and (d)–(f) $(00\bar{1})$ surface. Reprinted from *Appl. Surf. Sci.*, 469, C.L. Peng, Y.H. Zhong, G.S. Wang, F.F. Min, and L. Qin, Atomic-level insights into the adsorption of rare earth $Y(OH)_{3-n}^{n+}$ ($n = 1$–3) ions on kaolinite surface, 357-367, Copyright 2019, with permission from Elsevier.

MD and GCMC simulations can also be used to determine the properties of counterions to negative charge when two colloidal particles are adjacent to each other. In the separation of the two adjacent particles, the delamination of clay minerals, the location of interlayer cations, and the number of

water molecules surrounding the hydrated cations can be obtained [22,82]. The hydrated Na^+, K^+, or Cs^+ is located near the mid-plane of the interlayer space, and this cation hydration provides the energy for separation [82]. Conversely, when two colloidal particles approach each other, the cation

charge on the two surfaces cannot completely balance the surface potential because part of the counterions may be squeezed to the bulk area. This phenomenon causes about

20% charge imbalance at the separation distance of 1 Debye length and up to 80% if the separation decreases to 1/10 [83].
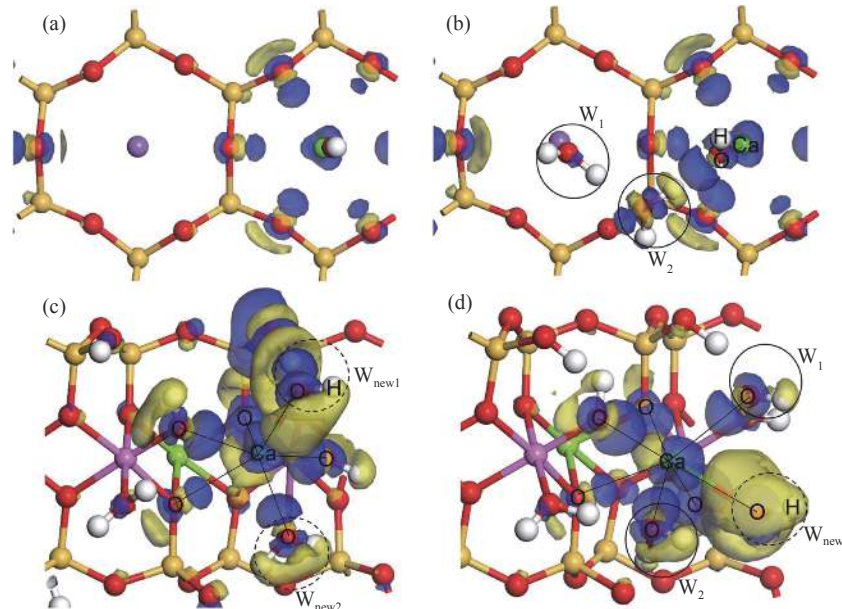
Fig. 3. **Electron density pattern of CaOH$^+$ adsorbed on Na-montmorillonite surfaces: (a) (001) surface–CaOH$^+$; (b) (001) surface–water–CaOH$^+$; (c) (010) surface–CaOH$^+$; (d) (010) surface–water–CaOH$^+$. W$_1$, W$_2$, W$_{new1}$ and W$_{new2}$, H, Ca, and O denote the first water, second water, new generated water molecules, hydrogen, calcium, and oxygen atoms, respectively. C.L. Peng, F.F. Min, L.Y. Liu, and J. Chen, *Surf. Interface Anal.*, 49, 267-277(2016) [17], Copyright Wiley-VCH Verlag GmbH & Co. KGaA. Reproduced with permission.**

4. Hydration

4.1. Surface hydration

The surface hydration repulsion force between two charged surfaces is not considered in the classic DLVO theory [84–86]. The strong short-range structure force induced by surface hydration can be detected by AFM colloid probe measurement even at extremely low ionic concentrations (Milli-Q water level) [87–88]. Meanwhile, the morphology of water molecular absorption on the surfaces and ions can be calculated by MD simulation. Then, the relationship between surface charge and hydration can be explained through experimental and simulation studies.

4.1.1. Experimental research on surface hydration

(1) Thickness measurements of the hydration layer

The thickness of the hydration layer is the most important parameter of the surface hydration layer. Numerous experimental methods can be used to measure the thickness of hydration layers. Recently, Mysels–Jones (MJ) experimental cell measurement, scanning transmission electron microscopy (STEM), and AFM have been used to measure the thickness of the hydration layer.

In MJ experimental cell measurement, which is also named as "thin film pressure balance measurement" [89], the

hydration force can be expressed by the dependence of the disjoining pressure on the film thickness [90]. The film forms in the center of a cylindrical hole of a porous-glass plate, which allows two film surfaces to be forced against each other at pressures greater than 7000 Pa. The film thickness can be measured by the intensity of the reflected light at the wavelength of 546 nm from the film [91–92]. This method can used to analyze the hydration layer in various dispersion systems at high cation concentrations [93].

The thickness of the hydration layer on borosilicate glass can also be detected by a combination of focused ion beam and STEM [93], and nanoindentation data on the surface of the same glass can be collected in quasi-static mode using a commercial Hysitron triboscope nanoindenter (Hysitron Inc., USA) equipped with a Berkovich tip. Experimental results showed that transmission electron microscopy provides a more direct measurement; however, the specimen preparation is complex [94].

The measurement method for hydration layer thickness also depends on the particle shape. The thickness of the hydration layer of plate-like particles can be detected by a combination of AFM and viscosity measurement. The method is based on the viscosity theory of dispersions of solid nanosheets. By using this method, the thickness of the slip-

ping layer of the hydration layer on montmorillonite (001) surface during motion was detected to be 1.63 nm [95].

(2) Property measurement of the hydration layer

The properties of the hydration layer can be characterized by various innovative designed experiments, such as the radiochemical method, vibrational spectra method, and AFM. The amount of water in the hydration layer can be measured using the radiochemical method. In this method, the surface is exchanged with tritiated water, and then back-exchange data are used as a parameter of the hydrated film thickness. The results show that the method is more sensitive than optical methods but is seriously temperature dependent [96].

The molecular behavior in the hydration layer can also detected by vibrational spectroscopy. Vibrational spectroscopy results suggest that the bulk properties of the aqueous solutions (e.g., pH value) affect the structure of the hydration layer [20,97–98]. Fig. 4 shows the infrared ray (IR)–visible sum-frequency generation spectral curves at 3200 and 3450 cm^{-1} detected at the Al_2O_3 surface when pH value is 3 and 12, respectively. Results indicate that the differences between the relative phases of these two spectra are 0.99π and 0.97π, respectively. This result means that the direction of H_2O dipoles on the sapphire (Al_2O_3) [97] and crystalline or fused surfaces is reversed when the pH crosses the IEP. A similar result was obtained on a quartz (SiO_2) surface [20]. In addition, the surface hydrated water molecules of quartz at low
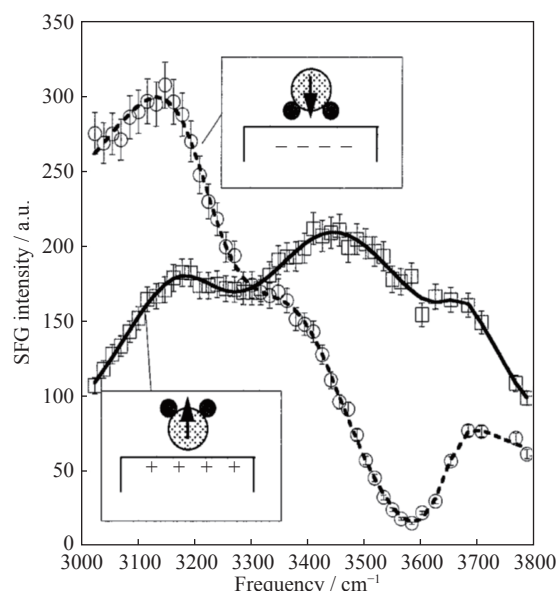
Fig. 4.   Sum-frequency generation (SFG) spectral curves at the Al_2O_3 interface when pH values are 3 and 12. [Fig. 1] reprinted with permission from [M.S. Yeganeh, S.M. Dougal, and H. S. Pink, *Phys. Rev. Lett.*, 83, 1179-1182 (1999) [97]. Copyright 1999 by the American Physical Society. Provide a hyperlink from the reprinted APS material for information, see https://doi.org/10.1103/PhysRevLett.83.1179 to obtain the link.

(2) and high (12) pH values are well ordered and exhibit spectroscopic features similar to the ice–quartz interface. At intermediate pH values, the hydration water is less ordered [20,99].

The structure of the hydration layer can also be detected using AFM [100]. The hydration force/structure remains oscillatory, even down to detect a single water molecule, and its lateral extent is limited to a size of a few water molecules. Between the tip and the spaceman, a layer of water molecules remains "bound" on the specimen surface during detection, which could reduce the lateral force [101–102]. By adjusting the distance between the specimen and the tip, the first and second hydration layers on the mica surface can be visualized by AFM, which gives honeycomb-like and dot-like patterns, respectively, as shown in Fig. 5 [102].

4.1.2. Simulation research on particle surface hydration

Simulation is a precise method that allows molecular-scale investigations. The hydration layer on different types of particle surfaces has been studied by simulation. The thickness of the hydration layer varies between different types of surfaces. Yi *et al*. [103] found through simulation that the thicknesses of the ordered and transition layers on the (001) surface of montmorillointe are 0.85 and 0.89 nm, respectively. The total thickness of the layer is 1.74 nm under static conditions, which is slightly thinner than that (1.63 nm) obtained by Zhao *et al*. [95] under shearing conditions. The two results support each other, but the principles of the methods in determining the thickness slightly differ. The thickness of the hydration layer derived by Yi *et al*. [103] was defined by the dipole orientation, whereas that in the study by Zhao *et al*. [95] was defined as the slipping layer. On the surface of brucite, the water molecules in the first hydration layer approximately 0.245 nm thick are well ordered. The translational ordering effect of the water layer extends to 0.5 nm, density effects to 1.0 nm, and orientational effects to 1.5 nm [104]. For the hydration layer on a protein, which is called "biological water," the oriented water molecules form approximately three to five hydration shells [105]. A two-component first monolayer (0.23 and 0.30 nm) and a second monolayer (0.50 nm) of the calcite mineral were detected on the surface of the mineral calcite [106]. Between two mica surfaces, a strong hydration force was detected when the distance was approximately 2.0 nm, and the repulsion force aroused by hydration layer was much stronger than that of EDL [107]. The hydration layer on the kaolinite surface consists of a 3-water-molecule layer approximately 0.8–1.0 nm thick [108].

The properties of the hydration layer also vary between different materials. The interactions between two basal kaolinite surfaces and water molecules are mainly of hydrogen bonds [108]. However, the electrostatic interaction dominates the montomorillonite basal surface [23]. The (00$\bar{1}$) surface of kaolinite has a greater adsorption energy for water molecules than the (001) surface [108]. Meanwhile, the edge
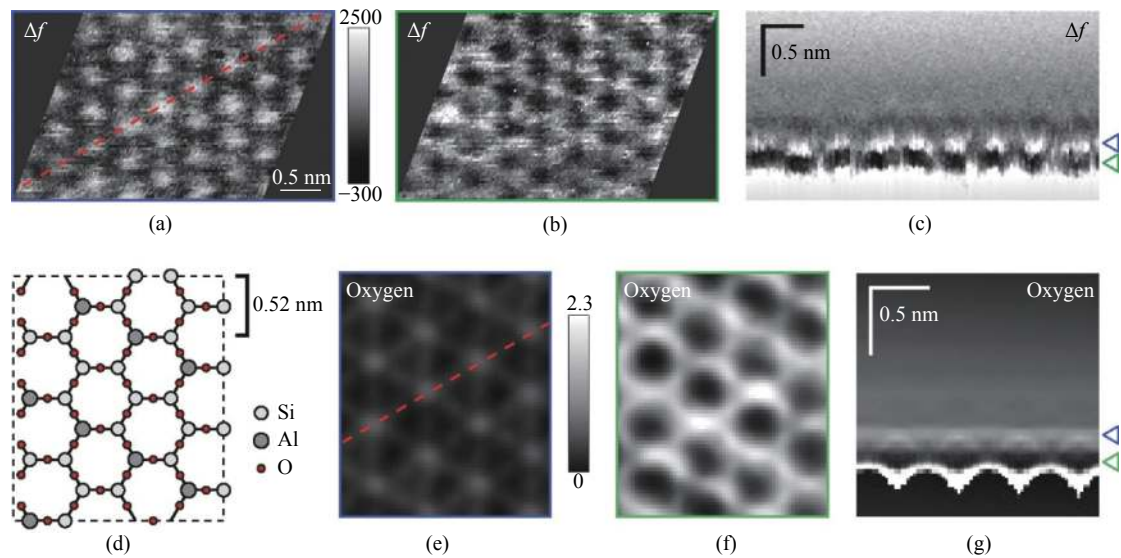
Fig. 5. (a, b) Two dimensions (2D) frequency shift maps (z–x slices) showing dot-like and honeycomb-like patterns. The honeycomb-like pattern was visualized when the tip was approached further by 0.2 nm to the surface from the tip-sample distance with the dot-like pattern. (c) 2D frequency shift map in the z–x plane including the dotted line in (a). The triangles on the right of the map represent the locations of the two x–y slices in (a) and (b). Δf is the frequency shift. (d) Schematic of surface atoms of the muscovite mica model used in the three dimensions reference interaction site model (3D-RISM) calculation. (e, f) Calculated 2D oxygen density maps showing dot-like and honeycomb-like features. (g) Calculated 2D oxygen density map in the z–x plane including the dotted line in (e). The triangles on the right of the map represent the locations of the two x–y slices in (e) and (f). Reprinted with permission from [K. Kobayashi, N. Oyabu, K. Kimura, S. Ido, and K. Suzuki, *J. Chem. Phys.*, 138, art. No. 184704 (2013) [102]. Copyright 2013 AIP Publishing LLC.

surface of montomorllonite has greater adsorption energy than the basal surface for water molecules [23]. For clay minerals, the hydration layer is composed of two contributions. The two-component behavior could be the result of the hydration shell structure being composed of two bound water layers [109]. Bourg and Sposito [110] investigated the hydration layer between two parallel smectite clay surfaces. The water molecules and ions diffuse relatively rapidly even in the first hydration layer, which contradicts with the reports of rigid "ice-like" hydrated water structures on clay surfaces. The author agrees with Bourg's "relatively diffuse" results, which concur with previous experimental research [25].

The interfacial water structure largely depends on surface chemistry; thus, large qualitative differences in the hydration layer exist between hydrophobic and hydrophilic surfaces [111]. The difference in density profiles has profound implications for the hydrodynamic properties of the interfacial layer [112]. The hydrodynamic boundary condition at solid–liquid interfaces depends decisively on the hydrophobicity of the surface and the associated water structure. At hydrophilic interfaces (e.g., glass fracture surface), the strongest adsorption sites are associated with coordination defects, and modifier species are weaker than coordination defects for the glass fracture surface [113]. Experiments measuring the hydrodynamic force on hydrophilic glass particles are compatible with a highly viscous interfacial water layer with a width of up to ~1 nm [114]. Simulations show

that the viscosity in the first water layers adjacent to hydrophilic surfaces exceeds the bulk viscosity [115–116]. At hydrophobic interfaces (e.g., graphene surface), the first hydrated water molecules have a good orientation with the surface normal, and its positioning is consistent with the local ice-like structure [117]. The fluid slips along the surface, which can be modeled using a finite slip length. The extent of slippage depends on the charge density [115] and roughness [116] of the solid surface and on the pressure, impurities, and dissolved gas in the liquid phase [118].

In summary, the structure of the water molecules in the hydration layer is mainly influenced by the pH value, surface hydrophobicity and ability to form H bonds with adsorbed water molecules, surface structure, surface charge types, and hydrolysis species. Meanwhile, the hydroxyl groups are more efficient than cations at structuring water adjacent to the surface for silica [8].

4.2. Ion hydration

Research on the effect of hydration on aggregation revealed a surprising stability in colloidal dispersions at high salt concentrations and pH value around the IEP, which cannot be modeled by classical DLVO theory [119]. AFM results confirmed that this stability is caused by the hydration forces induced by the accumulation of hydrated cations on the surface [120]. Thus, ion hydration is an important component of surface hydration.

An ion has a strong polarizing capability because of its high charge-to-radius ratio. It adsorbs the water molecules around it to form the hydration shell. The coordination numbers of Na^+, K^+, Mg^{2+}, and Ca^{2+} are 5.6, 6.7, 6.0, and 7.8, respectively [2]. Ion enforces the water molecules in its first hydration shell to serve solely as hydrogen bond donors between the first and second hydration shells [121]. Compared with the bulk water molecules, the water molecules treated quantum mechanically by ion plus first hydration shell show marginally shorter O–H bonds and wider H–O–H angles [122–123]. Meanwhile, the rotation frequencies of water molecules in the first shell are blueshifted [123]. This blueshift is different for different types of ions. Then, some cations (Na^+) can act as structure-making (or kosmotrope) ions that form strong hydrated complexes, whereas other cations (K^+) can be considered as disturbances around the surrounding environment, revealing the structure-breaking (or chaotrope) ability on the hydration shell [124]. The short-range hydration forces modify the interaction between oppositely charged ions. They enhance attraction between two kosmotropes or two chaotropes and induce short-range repulsion between two ions of opposite nature [30]. This principle was generalized by Gierst *et al*. [125] to surfaces. Similar ideas were later introduced by Collins [126–127] in his formulation of the "like seeks like." The thickness of the interfacial layer is strongly dependent on hydration shell size and hydration energy of surface ions. Majority of water molecules in the second contact surface hydrated layer hydrate the surface ions and together with the rest of the water molecules form hydrogen bonds among themselves. The structure of the water molecules in the third and subsequent layer is random and more bulk liquidlike, except those molecules that hydrate the surface ions [128].

5. Summary and conclusions

This review presented an extensive range of studies on surface charge and hydration, especially of some common minerals or material surfaces, covering experimental methods, theoretical studies, and simulation techniques to interpret the correlation between surface charge and hydration. The adsorption of hydrogen ions does not give rise to hydration forces; however, it affects the surface potential. The hydration effect can arise from the adsorption of cations. Meanwhile, the adsorption of cations and cation hydrolysis species can be raised from surface hydration. The effect of counterion hydration is different between different surface structures and ion valence. The difference between divalent and monovalent cations is that the hydration shell of latter is stronger and harder to shed than the former during adsorption.

With the development of colloid surface science, the use of the traditional DLVO theory for experimental phenomen-

on under specific conditions is inappropriate, in which a short-term repulsive force, the hydration force, becomes a non-negligible interaction between colloid particles. Hydration mainly includes two parts when particles are immersed in electrolyte solutions: surface hydration and surface ion hydration. Many influencing factors, such as ion concentration, ion type and valence, ion hydrolysis species, surface properties, and charge hydration asymmetry, impact/may impact the charge and hydration behavior.

The surface charge and hydration still needs to be systematically investigated to achieve a favorable surface theory for the correlation between surface charge and hydration. A solid and strong study on surface charge and hydration should have the following features.

(1) The study should be able to strengthen the theoretical foundation of the research of surface charge and hydration. Investigations of the correlation between surface hydration and charge have been broad, and many research methods were involved, including experimental investigations, computer simulations, formula models, DLVO theory, PB theory, and ion hydration. These investigations are interdependent and are expected to be combined to form a theoretical system. If one of these theories is improved, then the other theory should be correspondingly modified. For example, the charge behavior of ions on a surface is influenced by the diversity of the hydrolysis species and the ratio of them. Thus, the effect of hydrolysis of the ions should be considered in PB and DLVO theory.

(2) The study should establish the relation between ion hydration on the surface and in bulk water. First, the hydration structure varies between different types of ions and ion hydrolysis. A steric relationship must be established between ion hydration and surface hydration to determine the effect of different ion hydration conditions on surface charge and hydration. Second, the effects of ion hydration and surface charge in the inner and outer parts of the double layer should be clarified. The boundary of the compact and diffuse parts of the double layer changes with ion hydration. The relation between ion hydration, hydrolysis and co-ions in the interface, and theirs effect on the ion correlations behavior both in short range and long range should be studied.

(3) A novel detection method for hydration and charged layers needs to be invented. Currently, surface charge and hydration are detected using AFM and SFM. With the development of microscopic experiments, some macroscopic effects on the surface charge and hydration remain to be clarified by novel microscopic experiments. Limitations of the human exploration of the surface charge also need to be identified. Other important questions to be answered about the novel detection method include the following: What is the boundary between direct and indirect measurements? What model should be developed to broaden our sight? What real objects can be measured using a model? Can the detection be

performed in reality or what are the limitations in human exploration?

Acknowledgements

This work was financially supported by the National Natural Science Foundation of China (Nos. 51804213, 51820105006, 51474167, 51674183, and 51674174) and the China Scholarships Council (No. 201906935041).

References

[1]   E.I. Benítez, D.B. Genovese, and J.E. Lozano, Effect of pH and ionic strength on apple juice turbidity: Application of the extended DLVO theory, *Food Hydrocolloids*, 21(2007), No. 1, p. 100.

[2]   C.F. Liu, F.F. Min, L.Y. Liu, and J. Chen, Hydration properties of alkali and alkaline earth metal ions in aqueous solution: A molecular dynamics study, *Chem. Phys. Lett.*, 727(2019), p. 31.

[3]   F.F. Min, C.I. Peng, and S.X. Song, Hydration layers on clay mineral surfaces in aqueous solutions: A review, *Arch. Min. Sci.*, 59(2014), No. 2, p. 489.

[4]   R.M. Pashley, DLVO and hydration forces between mica surfaces in Li^+, Na^+, K^+, and Cs^+ electrolyte solutions: A correlation of double-layer and hydration forces with surface cation exchange properties, *J. Colloid Interface Sci.*, 83(1981), No. 2, p. 531.

[5]   G.A. Parks, The isoelectric points of solid oxides, solid hydroxides, and aqueous hydroxo complex systems, *Chem. Rev.*, 65(1965), No. 2, p. 177.

[6]   R.M. Pashley, Hydration forces between mica surfaces in electrolyte solutions, *Adv. Colloid Interface Sci.*, 16(1982), No. 1, p. 57.

[7]   R.M. Pashley and J.N. Israelachvili, DLVO and hydration forces between mica surfaces in Mg^{2+}, Ca^{2+}, Sr^{2+}, and Ba^{2+} chloride solutions, *J. Colloid Interface Sci.*, 97(1984), No. 2, p. 446.

[8]   J.P. Chapel, Electrolyte species dependent hydration forces between silica surfaces, *Langmuir*, 10(1994), No. 11, p. 4237.

[9]   A. Chandra, Dynamics of electrical double layer formation at a charged solid surface, *J. Mol. Struct.*, 430(1998), p. 105.

[10]   K.D. Collins and M.W. Washabaugh, The Hofmeister effect and the behaviour of water at interfaces, *Q. Rev. Biophys.*, 18(1985), No. 4, p. 323.

[11]   M.M. Hatlo, R. van Roij, and L. Lue, The electric double layer at high surface potentials: The influence of excess ion polarizability, *Europhys. Lett.*, 97(2012), No. 2, art. No. 28010.

[12]   M.E. Fleharty, F. Van Swol, and D.N. Petsev, Solvent role in the formation of electric double layers with surface charge regulation: A bystander or a key participant?, *Phys. Rev. Lett.*, 116(2016), No. 4, art. No. 048301.

[13]   S. Dewan, M.S. Yeganeh, and E. Borguet, Experimental correlation between interfacial water structure and mineral reactivity, *J. Phys. Chem. Lett.*, 4(2013), No. 11, p. 1977.

[14]   M. Holovko, M. Druchok, and T. Bryk, A molecular dynamics study of the hydrated–hydrolyzed structure of multivalent cations based on the model of primitive cation, *J. Mol. Liq.*, 131-132(2007), p. 65.

[15]   Q.Y. Hu, C. Weber, H.W. Cheng, F.U. Renner, and M. Valt-

iner, Anion layering and steric hydration repulsion on positively charged surfaces in aqueous electrolytes, *ChemPhysChem*, 18(2017), No. 21, p. 3056.

[16]   R. Scheu, B.M. Rankin, Y.X. Chen, K.C. Jena, D. Ben-Amotz, and S. Roke, Charge asymmetry at aqueous hydrophobic interfaces and hydration shells, *Angew. Chem. Int. Ed.*, 53(2014), No. 36, p. 9560.

[17]   C.L. Peng, F.F. Min, L.Y. Liu, and J. Chen, The adsorption of $CaOH^+$ on (001) basal and (010) edge surface of Na-montmorillonite: A DFT study, *Surf. Interface Anal.*, 49(2017), No. 4, p. 267.

[18]   C.F. Liu, F.F. Min, L.Y. Liu, and J. Chen, Density functional theory study of water molecule adsorption on the α-quartz (001) surface with and without the presence of Na^+, Mg^{2+}, and Ca^{2+}, *ACS Omega*, 4(2019), No. 7, p. 12711.

[19]   C.J. Van Oss, R.J. Good, and M.K. Chaudhury, The role of van der Waals forces and hydrogen bonds in "hydrophobic interactions" between biopolymers and low energy surfaces, *J. Colloid Interface Sci.*, 111(1986), No. 2, p. 378.

[20]   Q. Du, E. Freysz, and Y.R. Shen, Vibrational spectra of water molecules at quartz/water interfaces, *Phys. Rev. Lett.*, 72(1994), No. 2, p. 238.

[21]   S.X. Song, C.S. Peng, M.A. Gonzalez-Olivares, A. Lopez-Valdivieso, and T. Fort, Study on hydration layers near nanoscale silica dispersed in aqueous solutions through viscosity measurement, *J. Colloid Interface Sci.*, 287(2005), No. 1, p. 114.

[22]   A. Chatterjee, T. Iwasaki, T. Ebina, and A. Miyamoto, A DFT study on clay–cation–water interaction in montmorillonite and beidellite, *Comput. Mater. Sci.*, 14(1999), No. 1-4, p. 119.

[23]   C.L. Peng, F.F. Min, L.Y. Liu, and J. Chen, A periodic DFT study of adsorption of water on sodium-montmorillonite (001) basal and (010) edge surface, *Appl. Surf. Sci.*, 387(2016), p. 308.

[24]   H. Yi, F.F. Jia, Y.L. Zhao, W. Wang, S.X. Song, H.Q. Li, and C. Liu, Surface wettability of montmorillonite (001) surface as affected by surface charge and exchangeable cations: A molecular dynamic study, *Appl. Surf. Sci.*, 459(2018), p. 148.

[25]   H.L. Li, S.X. Song, Y.L. Zhao, Y. Nahmad, and T.X. Chen, Comparison study on the effect of interlayer hydration and solvation on montmorillonite delamination, *JOM*, 69(2017), No. 2, p. 254.

[26]   D.F. Parsons and B.W. Ninham, Surface charge reversal and hydration forces explained by ionic dispersion forces and surface hydration, *Colloids Surf. A*, 383(2011), No. 1-3, p. 2.

[27]   J.I. Kilpatrick, S.H. Loh, and S.P. Jarvis, Directly probing the effects of ions on hydration forces at interfaces, *J. Am. Chem. Soc.*, 135(2013), No. 7, p. 2628.

[28]   F.F. Min, C.L. Peng, and L.Y. Liu, Investigation on hydration layers of fine clay mineral particles in different electrolyte aqueous solutions, *Powder Technol.*, 283(2015), p. 368.

[29]   C.Y. Park, P.A. Fenter, K.L. Nagy, and N.C. Sturchio, Hydration and distribution of ions at the mica–water interface, *Phys. Rev. Lett.*, 97(2006), No. 1, art. No. 016101.

[30]   J. Morag, M. Dishon, and U. Sivan, The governing role of surface hydration in ion specific adsorption to silica: An AFM-based account of the Hofmeister universality and its reversal, *Langmuir*, 29(2013), No. 21, p. 6317.

[31]   Y.Z. Li, C. Zhang, Y.P. Jiang, T.J. Wang, and H.F. Wang, Effects of the hydration ratio on the electrosorption selectivity of ions during capacitive deionization, *Desalination*, 399(2016), p. 171.

[32]   D.F. Parsons and A. Salis, Hofmeister effects at low salt concentration due to surface charge transfer, *Curr. Opin. Colloid*

Interface Sci., 23(2016), p. 41.

[33] S. Veeramasuneni, Y.H. Hu, M.R. Yalamanchili, and J.D. Miller, Interaction forces at high ionic strengths: The role of polar interfacial interactions, *J. Colloid Interface Sci.*, 188(1997), No. 2, p. 473.

[34] H.J. Butt, Electrostatic interaction in atomic force microscopy, *Biophys. J.*, 60(1991), No. 4, p. 777.

[35] A. Grabbe and R.G. Horn, Double-layer and hydration forces measured between silica sheets subjected to various surface treatments, *J. Colloid Interface Sci.*, 157(1993), No. 2, p. 375.

[36] Z. Zachariah, R.M. Espinosa-Marzal, and M.P. Heuberger, Ion specific hydration in nano-confined electrical double layers, *J. Colloid Interface Sci*, 506(2017), p. 263.

[37] T. Baimpos, B.R. Shrestha, S. Raman, and M. Valtiner, Effect of interfacial ion structuring on range and magnitude of electric double layer, hydration, and adhesive interactions between mica surfaces in 0.05–3 M Li$^+$ and Cs$^+$ electrolyte solutions, *Langmuir*, 30(2014), No. 15, p. 4322.

[38] P.F. Low, Influence of adsorbed water on exchangeable ion movement, *Clays Clay Miner.*, 9(1960), No. 1, p. 219.

[39] M. Manciu and E. Ruckenstein, Specific ion effects via ion hydration: I. Surface tension, *Adv. Colloid Interface Sci.*, 105(2003), No. 1-3, p. 63.

[40] H.H. Huang and E. Ruckenstein, Effect of hydration of ions on double-layer repulsion and the hofmeister series, *J. Phys. Chem. Lett.*, 4(2013), No. 21, p. 3725.

[41] S.J. Miklavic and B.W. Ninham, Competition for adsorption sites by hydrated ions, *J. Colloid Interface Sci.*, 134(1990), No. 2, p. 305.

[42] P.M. Biesheuvel and M. van Soestbergen, Counterion volume effects in mixed electrical double layers, *J. Colloid Interface Sci.*, 316(2007), No. 2, p. 490.

[43] H.J. Butt, Measuring local surface charge densities in electrolyte solutions with a scanning force microscope, *Biophys. J.*, 63(1992), No. 2, p. 578.

[44] N. Cuvillier and F. Rondelez, Breakdown of the Poisson–Boltzmann description for electrical double layers involving large multivalent ions, *Thin Solid Films*, 327-329(1998), p. 19.

[45] J. Sotres, A. Lostao, C. Gómez-Moreno, and A.M. Baró, Jumping mode AFM imaging of biomolecules in the repulsive electrical double layer, *Ultramicroscopy*, 107(2007), No. 12, p. 1207.

[46] W.F. Heinz and J.H. Hoh, Relative surface charge density mapping with the atomic force microscope, *Biophys. J.*, 76(1999), No. 1, p. 528.

[47] T. Hiemstra and W.H. Van Riemsdijk, On the relationship between charge distribution, surface hydration, and the structure of the interface of metal hydroxides, *J. Colloid Interface Sci.*, 301(2006), No. 1, p. 1.

[48] X.H. Yin, V. Gupta, H. Du, X.M. Wang, and J.D. Miller, Surface charge and wetting characteristics of layered silicate minerals, *Adv. Colloid Interface Sci.*, 179-182(2012), p. 43.

[49] J. Liu, L. Sandaklie-Nikolova, X.M. Wang, and J.D. Miller, Surface force measurements at kaolinite edge surfaces using atomic force microscopy, *J. Colloid Interface Sci.*, 420(2014), p. 35.

[50] T.X. Chen, Y.L. Zhao, H.L. Li, J. Liu, and S.X. Song, Electrokinetic characteristics of calcined kaolinite in aqueous electrolytic solutions, *Surf. Rev. Lett.*, 22(2015), No. 3, art. No. 1550041.

[51] P. Sinha, I. Szilagyi, F.J. Montes Ruiz-Cabello, P. Maroni, and M. Borkovec, Attractive forces between charged colloidal particles induced by multivalent ions revealed by confronting aggregation and direct force measurements, *J. Phys. Chem. Lett.*, 4(2013), No. 4, p. 648.

[52] A.W. Adamson, *Physical Chemistry of Surfaces*, John Wiley & Sons Inc., New York, 1990, p. 134.

[53] B.V. Derjaguin and S.S. Dukhin, Theory of flotation of small and medium-size particles, *Prog. Surf. Sci.*, 43(1993), No. 1-4, p. 241.

[54] D. Andelman, Electrostatic properties of membranes: the Poisson-Boltzmann theory, [in] R. Lipowsky and E. Sackmann, eds., *Handbook of Biological Physics*, Elsevier, Nederland, 1995, p. 603.

[55] I. Borukhov, D. Andelman, and H. Orland, Adsorption of large ions from an electrolyte solution: A modified Poisson–Boltzmann equation, *Electrochim. Acta*, 46(2000), No. 2-3, p. 221.

[56] X.M. Liu, H. Li, R. Li, and R. Tian, Analytical solutions of the nonlinear Poisson–Boltzmann equation in mixture of electrolytes, *Surf. Sci.*, 607(2013), p. 197.

[57] P.H. R. Alijó, F.W. Tavares, and E.C. Biscaia Jr, Double layer interaction between charged parallel plates using a modified Poisson–Boltzmann equation to include size effects and ion specificity, *Colloids Surf. A*, 412(2012), p. 29.

[58] D. Ben-Yaakov and D. Andelman, Revisiting the Poisson–Boltzmann theory: Charge surfaces, multivalent ions and inter-plate forces, *Physica A*, 389(2010), No. 15, p. 2956.

[59] J.P. Hsu, H.Y. Yu, and S. Tseng, Approximate analytical expressions for the electrical potential between two planar, cylindrical, and spherical surfaces, *J. Phys. Chem. B*, 110(2006), No. 49, p. 25007.

[60] J.P. Hsu and C.H. Huang, Electrical potentials of two identical planar, cylindrical, and spherical colloidal particles in a salt-free medium, *J. Colloid Interface Sci.*, 348(2010), No. 2, p. 402.

[61] J. Stankovich and S.L. Carnie, Interactions between two spherical particles with nonuniform surface potentials: The linearized Poisson–Boltzmann theory, *J. Colloid Interface Sci.*, 216(1999), No. 2, p. 329.

[62] J.K. Wang, M.R. Wang, and Z.X. Li, Lattice evolution solution for the nonlinear Poisson–Boltzmann equation in confined domains, *Commun. Nonlinear Sci. Numer. Simul.*, 13(2008), No. 3, p. 575.

[63] L.C. Liu and I. Neretnieks, Homo-interaction between parallel plates at constant charge, *Colloids Surf. A*, 317(2008), No. 1-3, p. 636.

[64] R. Kjellander, T. Åkesson, B. Jönsson, and S. Marčelja, Double layer interactions in mono and divalent electrolytes: A comparison of the anisotropic HNC theory and Monte Carlo simulations, *J. Chem. Phys.*, 97(1992), No. 2, p. 1424.

[65] S. Kewalramani, G.I. Guerrero-García, L.M. Moreau, J.W. Zwanikken, C.A. Mirkin, M.O. de La Cruz, and M.J. Bedzyk, Electrolyte-mediated assembly of charged nanoparticles, *ACS Cent. Sci.*, 2(2016), No. 4, p. 219.

[66] G.I. Guerrero-García, E. González-Tovar, M. Lozada-Cassou, and F. de J. Guevara-Rodríguez, The electrical double layer for a fully asymmetric 895 electrolyte around a spherical colloid?: An integral equation study, *J. Chem. Phys.*, 123(2005), No. 3, art. No. 034703.

[67] G.I. Guerrero-García, E. González-Tovar, and M. Chávez-Páez, Simulational and theoretical study of the spherical electrical double layer for a size-asymmetric electrolyte: The case of big coions, *Phys. Rev. E*, 80(2009), No. 2, art. No. 021501.

[68] G.I. Guerrero-García, E. González-Tovar, and M.O. de la

Cruz, Effects of the ionic size-asymmetry around a charged nanoparticle: Unequal charge neutralization and electrostatic screening, *Soft Matter*, 6(2010), No. 9, p. 2056.

[69] G.I. Guerrero-García, E. González-tovar, and M.O. de la Cruz, Entropic effects in the electric double layer of model colloids with size-asymmetric 907 monovalent ions, *J. Chem. Phys.*, 135(2011), No. 5, art. No. 054701.

[70] G.I. Guerrero-García, P. González-Mozuelos, and M.O. de la Cruz, Potential of mean force between identical charged nanoparticles immersed in a size-asymmetric monovalent electrolyte, *J. Chem. Phys.*, 135(2011), No. 16, art. No. 164705.

[71] G.I. Guerrero-García and M.O. de la Cruz, Inversion of the electric field at the electrified liquid–liquid interface, *J. Chem. Theory Comput.*, 9(2013), No. 1, p. 1.

[72] G.I. Guerrero-García, Y.F. Jing, and M.O. de la Cruz, Enhancing and reversing the electricfield at the oil–water interface with size-asymmetric monovalent ions, *Soft Matter*, 9(2013), No. 26, p. 6046.

[73] Z. Ovanesyan, B. Medasani, M.O. Fenley, G.I. Guerrero-García, M.O. de la Cruz, and M. Marucho, Excluded volume and ion–ion correlation effects on the ionic atmosphere around B-DNA: Theory, simulations, and experiments, *J. Chem. Phys.*, 141(2014), No. 22, art. No. 225103.

[74] G.I. Guerrero-García, E. González-Tovar, M. Quesada-Pérez, and A. Martín-Molina, The non-dominance of counterions in charge asymmetric electrolytes: Non-monotonic precedence of the electrostatic screening and local inversion of the electric field by multivalent coions, *Phys. Chem. Chem. Phys.*, 18(2016), No. 31, p. 21852.

[75] G.I. Guerrero-García, P. Gonzalez-Mozuelos, and M.O. de la Cruz, Large counterions boost the solubility and renormalized charge of suspended nanoparticles, *ACS Nano*, 7(2013), No. 11, p. 9714.

[76] G.I. Guerrero-García and M.O. de la Cruz, Polarization effects of dielectric nanoparticles in aqueous charge-asymmetric electrolytes, *J. Phys. Chem. B*, 118(2014), No. 29, p. 8854.

[77] G.I. Guerrero-García, E. González-Tovar, M. Chávez-Páez, J. Kłos, and S. Lamperski, Quantifying the thickness of the electrical double layer neutralizing a planar electrode: The capacitive compactness, *Phys. Chem. Chem. Phys.*, 20(2018), No. 1, p. 262.

[78] G.I. Guerrero-García, E. González-Tovar, M. Chávez-Páez, and T. Wei, Expansion and shrinkage of the electrical double layer in charge-asymmetric electrolytes: A non-linear Poisson–Boltzmann description, *J. Mol. Liq.*, 277(2019), p. 104.

[79] E. González-Tovar, F. Jiménez-Ángeles, R. Messina, and M. Lozada-Cassou, A new correlation effect in the Helmholtz and surface potentials of the electrical double layer, *J. Chem. Phys.*, 120(2004), No. 20, p. 9782.

[80] C.L. Moraila-Martínez, G.I. Guerrero-García, M. Chávez-Páez, and E. González-Tovar, An experimental/theoretical method to measure the capacitive compactness of an aqueous electrolyte surrounding a spherical charged colloid, *J. Chem. Phys.*, 148(2018), No. 15, art. No. 154703.

[81] C.L. Peng, Y.H. Zhong, G.S. Wang, F.F. Min, and L. Qin, Atomic-level insights into the adsorption of rare earth $Y(OH)_{3-n}^{n+}$ ($n = 1–3$) ions on kaolinite surface, *Appl. Surf. Sci.*, 469(2019), p. 357.

[82] H.L. Li, S.X. Song, X.S. Dong, F.F. Min, Y.L. Zhao, C.L. Peng, and Y. Nahmad, Molecular dynamics study of crystalline swelling of montmorillonite as affected by interlayer cation hydration, *JOM*, 70(2018), No. 4, p. 479.

[83] A. Torres, R. van Roij, and G. Téllez, Finite thickness and charge relaxation in double-layer interactions, *J. Colloid Interface Sci.*, 301(2006), No. 1, p. 176.

[84] V.N. Paunov, R.I. Dimova, P.A. Kralchevsky, G. Broze, and A. Mehreteab, The hydration repulsion between charged surfaces as an interplay of volume exclusion and dielectric saturation effects, *J. Colloid Interface Sci.*, 182(1996), No. 1, p. 239.

[85] J.J. Adler, Y.I. Rabinovich, and B.M. Moudgil, Origins of the non-DLVO force between glass surfaces in aqueous solution, *J. Colloid Interface Sci.*, 237(2001), No. 2, p. 249.

[86] H.H. Liu, J. Lanphere, S. Walker, and Y. Cohen, Effect of hydration repulsion on nanoparticle agglomeration evaluated via a constant number Monte–Carlo simulation, *Nanotechnology*, 26(2015), No. 4, art. No. 045708.

[87] S. Veeramasuneni, M.R. Yalamanchili, and J.D. Miller, Interactions between dissimilar surfaces in high ionic strength solutions as determined by atomic force microscopy, *Colloids Surf. A*, 131(1998), No. 1-3, p. 77.

[88] J.M. Duan, Interfacial forces between silica surfaces measured by atomic force microscopy, *J. Environ. Sci.*, 21(2009), No. 1, p. 30.

[89] N. Schelero, G. Hedicke, P. Linse, and R.V. Klitzing, Effects of counterions and co-ions on foam films stabilized by anionic dodecyl sulfate, *J. Phys. Chem. B*, 114(2010), No. 47, p. 15523.

[90] K.J. Mysels and M.N. Jones, Direct measurement of the variation of double-layer repulsion with distance, *Discuss. Faraday Soc.*, 42(1966), p. 42.

[91] A. Sheludko, Thin liquid films, *Adv. Colloid Interface Sci*, 1(1967), No. 4, p. 391.

[92] V. Bergeron and C.J. Radke, Equilibrium measurements of oscillatory disjoining pressures in aqueous foam films, *Langmuir*, 8(1992), No. 12, p. 3020.

[93] P.A. Kralchevsky, K.D. Danov, and E.S. Basheva, Hydration force due to the reduced screening of the electrostatic repulsion in few-nanometer-thick films, *Curr. Opin. Colloid Interface Sci.*, 16(2011), No. 6, p. 517.

[94] D.R. Tadjiev, R.J. Hand, and P. Zeng, Comparison of glass hydration layer thickness measured by transmission electron microscopy and nanoindentation, *Mater. Lett.*, 64(2010), No. 9, p. 1041.

[95] Y.L. Zhao, H. Yi, F.F. Jia, H.L. Li, C.S. Peng, and S.X. Song, A novel method for determining the thickness of hydration shells on nanosheets: A case of montmorillonite in water, *Powder Technol.*, 306(2017), p. 74.

[96] J.P. Lowe, D.J. Lowe, A.P.W. Hodder, and A.T. Wilson, A tritium-exchange method for obsidian hydration shell measurement, *Chem. Geol.*, 46(1984), No. 4, p. 351.

[97] M.S. Yeganeh, S.M. Dougal, and H.S. Pink, Vibrational spectroscopy of water at liquid/solid interfaces: Crossing the isoelectric point of a solid surface, *Phys. Rev. Lett.*, 83(1999), No. 6, p. 1179.

[98] V. Ostroverkhov, G.A. Waychunas, and Y.R. Shen, Vibrational spectra of water at water/α-quartz (0001) interface, *Chem. Phys. Lett.*, 386(2004), No. 1-3, p. 144.

[99] A.J. Hopkins, C.L. McFearin, and G.L. Richmond, Investigations of the solid–aqueous interface with vibrational sum-frequency spectroscopy, *Curr. Opin. Solid State Mater. Sci.*, 9(2005), No. 1-2, p. 19.

[100] K. Miyazawa, N. Kobayashi, M. Watkins, A.L. Shluger, K.I. Amanod, and T. Fukuma, A relationship between three-dimensional surface hydration structures and force distribution measured by atomic force microscopy, *Nanoscale*, 8(2016),

No. 13, p. 7334.

[101] R. Ho, J.Y. Yuan, and Z.F. Shao, Hydration force in the atomic force microscope: A computational study, *Biophys. J.*, 75(1998), No. 2, p. 1076.

[102] K. Kobayashi, N. Oyabu, K. Kimura, S. Ido, K. Suzuki, T. Imai, K. Tagami, M. Tsukada, and H. Yamada, Visualization of hydration layers on muscovite mica in aqueous solution by frequency-modulation atomic force microscopy, *J. Chem. Phys.*, 138(2013), No. 18, art. No. 184704.

[103] H. Yi, X. Zhang, Y.L. Zhao, L.Y. Liu, and S.X. Song, Molecular dynamics simulations of hydration shell on montmorillonite (001) in water, *Surf. Interface Anal.*, 48(2016), No. 9, p. 976.

[104] J.W. Wang, A.G. Kalinichev, and R.J. Kirkpatrick, Molecular modeling of water structure in nano-pores between brucite (001) surfaces, *Geochimi. Cosmochim. Acta*, 68(2004), No. 16, p. 3351.

[105] D.R. Martin and D.V. Matyushov, Hydration shells of proteins probed by depolarized light scattering and dielectric spectroscopy: Orientational structure is significant, positional structure is not, *J. Chem. Phys*, 141(2014), No. 22, art. No. 22D501.

[106] T.D. Perry, R.T. Cygan, and R. Mitchell, Molecular models of a hydrated calcite mineral surface, *Geochim. Cosmochim. Acta*, 71(2007), No. 24, p. 5876.

[107] Y.S. Leng, Hydration force between mica surfaces in aqueous KCl electrolyte solution, *Langmuir*, 28(2012), No. 12, p. 5339.

[108] J. Chen, F.F. Min, L.Y. Liu, and C.F. Liu, Mechanism research on surface hydration of kaolinite, insights from DFT and MD simulations, *Appl. Surf. Sci.*, 476(2019), p. 6.

[109] L. Duponchel, S. Laurette, B. Hatirnaz, A. Treizebre, F. Affouard, and B. Bocquet, Terahertz microfluidic sensor for *in situ* exploration of hydration shell of molecules, *Chemom. Intell. Lab. Syst.*, 123(2013), p. 28.

[110] I.C. Bourg and G. Sposito, Molecular dynamics simulations of the electrical double layer on smectite surfaces contacting concentrated mixed electrolyte (NaCl–CaCl$_2$) solutions, *J. Colloid Interface Sci.*, 360(2011), No. 2, p. 701.

[111] D.J. Bonthuis and R.R. Netz, Beyond the continuum: How molecular solvent structure affects electrostatics and hydrodynamics at solid-electrolyte interfaces, *J. Phys. Chem. B*, 117(2013), No. 39, p. 11397.

[112] T. López-León, M.J. Santander-Ortega, J.L. Ortega-Vinuesa, and D.L. Bastos-González, Hofmeister effects in colloidal systems: Influence of the surface nature, *J. Phys. Chem. C*, 112(2008), No. 41, p. 16060.

[113] E.A. Leed and C.G. Pantano, Computer modeling of water adsorption on silica and silicate glass fracture surfaces, *J. Non-Cryst. Solids*, 325(2003), No. 1-3, p. 48.

[114] C.D.F. Honig and W.A. Ducker, No-slip hydrodynamic boundary condition for hydrophilic particles, *Phys. Rev. Lett.*, 98(2007), No. 2, art. No. 028305.

[115] L. Joly, C. Ybert, E. Trizac, and L. Bocquet, Liquid friction on charged surfaces: From hydrodynamic slippage to electrokinetics, *J. Chem. Phys.*, 125(2006), No. 20, art. No. 204716.

[116] C. Sendner, D. Horinek, L. Bocquet, and R.R. Netz, Interfacial water at hydrophobic and hydrophilic surfaces: Slip, viscosity, and diffusion, *Langmuir*, 25(2009), No. 18, p. 10768.

[117] L.M. Alarcón, D.C. Malaspina, E.P. Schulz, M.A. Frechero, and G.A. Appignanesi, Structure and orientation of water molecules at model hydrophobic surfaces with curvature: From graphene sheets to carbon nanotubes and fullerenes, *Chem. Phys.*, 388(2011), No. 1-3, p. 47.

[118] G.D. Smith, J.E. Swain, and C.L. Bormann, Microfluidics for gametes, embryos, and embryonic stem cells, *Semin. Reprod. Med.*, 29(2011), No. 1, p. 5.

[119] Y.I. Chang and P.K. Chang, The role of hydration force on the stability of the suspension of *Saccharomyces cerevisiae*—Application of the extended DLVO theory, *Colloids Surf. A*, 211(2002), No. 1, p. 67.

[120] J.J. Valle-Delgado, J.A. Molina-Bolívar, F. Galisteo-González, and M.J. Gálvez-Ruiz, Evidence of hydration forces between proteins, *Curr. Opin. Colloid Interface Sci.*, 16(2011), No. 6, p. 572.

[121] A. Bhattacharjee, A.B. Pribil, B.R. Randolf, B.M. Rode, and T.S. Hofer, Hydration of Mg^{2+} and its influence on the water hydrogen bonding network via ab initio QMCF MD, *Chem. Phys. Lett.*, 536(2012), p. 39.

[122] S.J. Suresh, K. Kapoor, S. Talwar, and A. Rastogi, Internal structure of water around cations, *J. Mol. Liq.*, 174(2012), p. 135.

[123] C. Kritayakornupong, K. Plankensteiner, and B.M. Rode, Dynamics in the hydration shell of Hg^{2+} ion: Classical and *ab initio* QM/MM molecular dynamics simulations, *Chem. Phys. Lett.*, 371(2003), No. 3-4, p. 438.

[124] A. Tongraar and B.M. Rode, Dynamical properties of water molecules in the hydration shells of Na$^+$ and K$^+$: *Ab initio* QM/MM molecular dynamics simulations, *Chem. Phys. Lett.*, 385(2004), No. 5-6, p. 378.

[125] L. Gierst, L. Vandenberghen, E. Nicolas, and A. Fraboni, Ion pairing mechanisms in electrode processes, *J. Electrochem. Soc.*, 113(1966), No. 10, p. 1025.

[126] K.D. Collins, Ions from the Hofmeister series and osmolytes: Effects on proteins in solution and in the crystallization process, *Methods*, 34(2004), No. 3, p. 300.

[127] K.D. Collins, Charge density-dependent strength of hydration and biological structure, *Biophys. J.*, 72(1997), No. 1, p. 65.

[128] S. Adapa, D.R. Swamy, S. Kancharla, S. Pradhan, and A. Malani, Role of mono- and divalent surface cations on the structure and adsorption behavior of water on mica surface, *Langmuir*, 34(2018), No. 48, p. 14472.